

2022-07-15

Analytical results for phase bunching in the pendulum model of wave-particle interactions

J. Albert, A. Artemyev, W. Li, L. Gan, Q. Ma. 2022. "Analytical results for phase bunching in the pendulum model of wave-particle interactions" *Front. Astron. Space Sci.*. <https://doi.org/10.3389/fspas.2022.971358>
<https://hdl.handle.net/2144/46484>

Downloaded from DSpace Repository, DSpace Institution's institutional repository



OPEN ACCESS

EDITED BY

Xiao-Jia Zhang,
University of California, Los Angeles,
United States

REVIEWED BY

Oliver Allanson,
University of Exeter, United Kingdom
Yikai Hsieh,
Kyoto University, Japan

*CORRESPONDENCE

Jay M. Albert,
jay.albert@us.af.mil

SPECIALTY SECTION

This article was submitted to Space
Physics,
a section of the journal
Frontiers in Astronomy and Space
Sciences

RECEIVED 17 June 2022

ACCEPTED 15 July 2022

PUBLISHED 11 August 2022

CITATION

Albert JM, Artemyev A, Li W, Gan L and
Ma Q (2022), Analytical results for phase
bunching in the pendulum model of
wave-particle interactions.
Front. Astron. Space Sci. 9:971358.
doi: 10.3389/fspas.2022.971358

COPYRIGHT

© 2022 Albert, Artemyev, Li, Gan and
Ma. This is an open-access article
distributed under the terms of the
[Creative Commons Attribution License
\(CC BY\)](https://creativecommons.org/licenses/by/4.0/). The use, distribution or
reproduction in other forums is
permitted, provided the original
author(s) and the copyright owner(s) are
credited and that the original
publication in this journal is cited, in
accordance with accepted academic
practice. No use, distribution or
reproduction is permitted which does
not comply with these terms.

Analytical results for phase bunching in the pendulum model of wave-particle interactions

Jay M. Albert ^{1*}, Anton Artemyev ², Wen Li ³, Longzhi Gan ³ and Qianli Ma ^{3,4}

¹Air Force Research Laboratory, Kirtland AFB, Rio Rancho, NM, United States, ²Department of Earth, Planetary, and Space Sciences, University of California, Los Angeles, Los Angeles, CA, United States, ³Center for Space Physics, Boston University, Boston, MA, United States, ⁴Department of Atmospheric and Oceanic Sciences, University of California, Los Angeles, Los Angeles, CA, United States

Radiation belt electrons are strongly affected by resonant interactions with cyclotron-resonant waves. In the case of a particle passing through resonance with a single, coherent wave, a Hamiltonian formulation is advantageous. With certain approximations, the Hamiltonian has the same form as that for a plane pendulum, leading to estimates of the change at resonance of the first adiabatic invariant I , energy, and pitch angle. In the case of large wave amplitude (relative to the spatial variation of the background magnetic field), the resonant change in I and its conjugate phase angle ξ are not diffusive but determined by nonlinear dynamics. A general analytical treatment of slow separatrix crossing has long been available and can be used to give the changes in I associated with “phase bunching,” including the detailed dependence on ξ , in the nonlinear regime. Here we review this treatment, evaluate it numerically, and relate it to previous analytical results for nonlinear wave-particle interactions. “Positive phase bunching” can occur for some particles even in the pendulum Hamiltonian approximation, though the fraction of such particles may be exponentially small.

KEYWORDS

wave-particle interactions, radiation belts, nonlinear, hamiltonian, test particle simulation

1 Introduction

Cyclotron-resonant interactions with whistler mode waves are of major importance for the dynamics of radiation belt electrons (Bortnik and Thorne, 2007). Many numerical studies of test particles interacting with coherent, monochromatic waves in an inhomogeneous background magnetic field have demonstrated that cyclotron-resonant interactions lead to changes in particle energy and pitch angle, due to the breaking of an adiabatic invariant (Chang and Inan, 1983; Bortnik et al., 2008). For sufficiently small amplitude waves these changes are diffusive, associated with a random wave-particle phase (Albert, 2010), but larger waves induce systematic, asymmetric changes, whose detailed behavior can be described in terms of phase bunching and phase trapping (Albert, 1993). Estimates of the associated energy and pitch angle ranges of

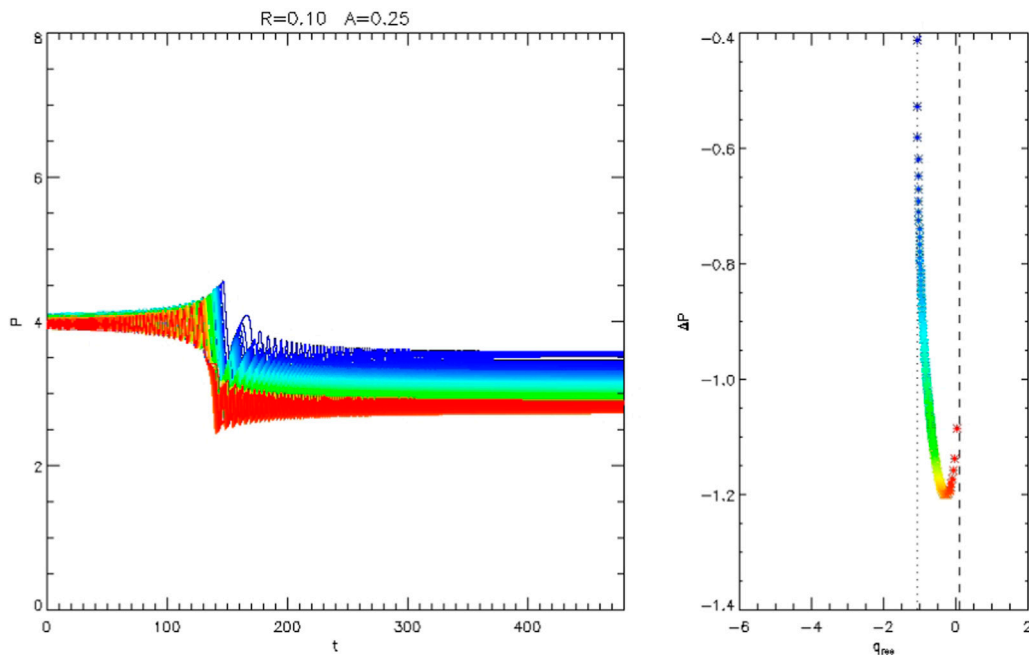


FIGURE 1

Trajectories of 120 particles from numerical integration of the equations of motion specified by the Hamiltonian of Eq. 11, with inhomogeneity parameter $R = 0.1$ and wave amplitude parameter $A = 0.25$. Left: P vs. t , showing systematic decrease associated with phase bunching at resonance. In this case, all values of ΔP are negative. Right: Change in P vs. the value of q at resonance. The dotted and dashed vertical lines show the calculated values q_{turn} and $q_x + 2\pi$, respectively, as discussed in the text.

such electrons have been given by, e.g., Albert (2002) and Albert et al. (2021). These processes are in turn deeply connected to nonlinear wave generation or growth (Omura et al., 2008).

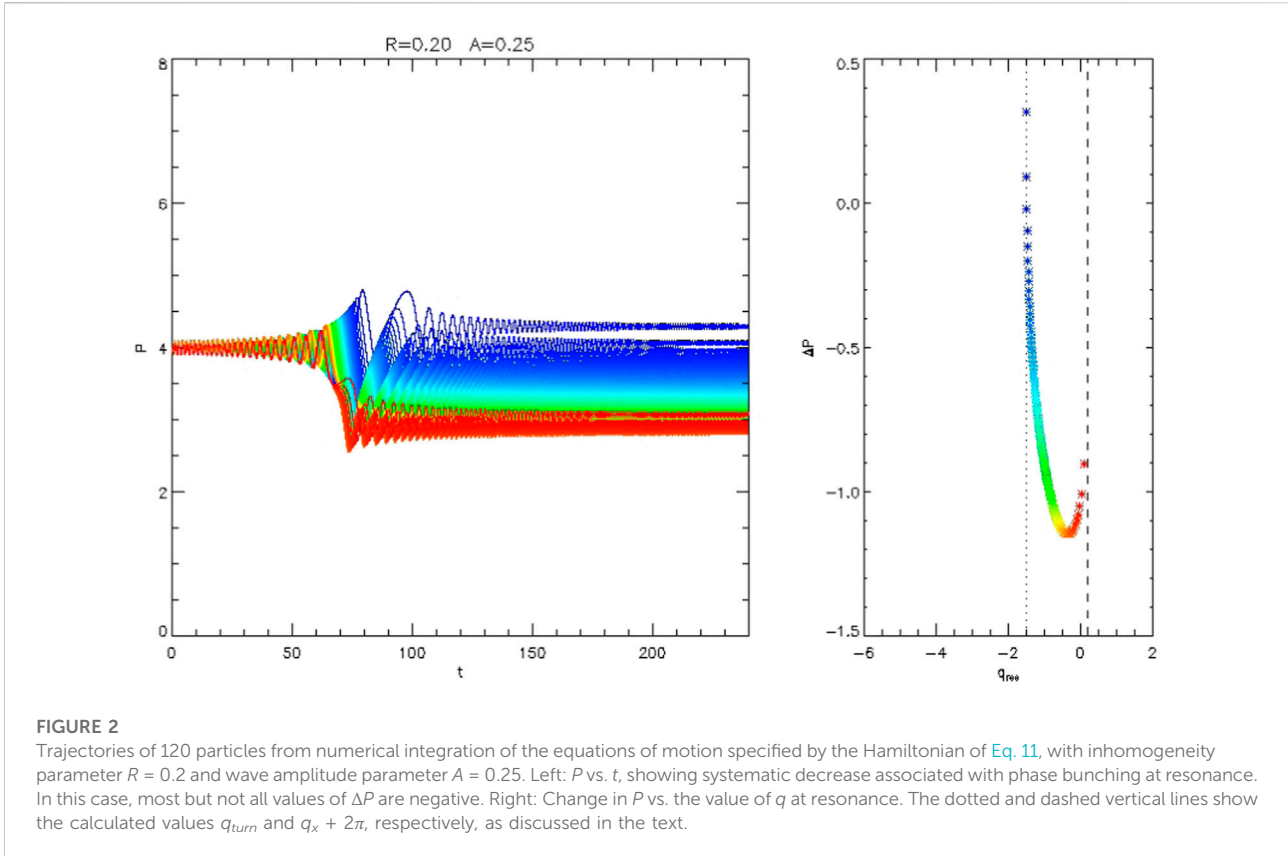
For electrons interacting with parallel-propagating whistler mode waves, phase trapping causes a sustained increase in particle energy and pitch angle, while phase bunching (that is, without trapping) causes these quantities to decrease; the lost particle energy can feed wave growth. Theory and simulation indicate that for representative wave and particle parameters, phase bunching has much higher probability than phase trapping in each resonant interaction. Typical particle trajectories showing phase bunching, obtained with a Hamiltonian formulation to be discussed below, are shown in Figures 1, 2. The variables P and q , defined in Section 3, are related, respectively, to the first adiabatic invariant I and its conjugate phase ξ , which are reviewed in Section 2.

Albert (1993) obtained an analytical estimate of the change in the first adiabatic invariant (and therefore energy and pitch angle) caused by phase bunching in the highly nonlinear limit, though the dependence on resonant wave-particle phase seen in numerical simulations was not accounted for. A more detailed expression can be written formally as an explicit but infinite and intractable integral, which must still be evaluated

numerically; however, averaging over the appropriate phase and interchanging integrals leads to a much more manageable expression (Neishtadt, 1999); this is presented in Section 4. Furthermore, the very general treatment of adiabatic invariant changes of Cary et al. (1986) can be applied to this problem, leading to a detailed and reliable approximation that retains the phase dependence in closed form. This treatment quantitatively captures the numerical observation that phase bunching-induced changes exhibit a spread of values, including some that are in fact in the positive direction. This is discussed in Section 5. Depending on the parameters used, adiabatic invariant increase may be physically significant yet too infrequent to detect from direct numerical simulation with a small number of particles.

2 Hamiltonian formulation

Albert (1993) and Albert (2000) derived a Hamiltonian $\mathcal{K}(I, \xi, z)$ appropriate for motion near a resonance. Recapping the definitions and results of those papers, equations of motion for the normalized first adiabatic invariant $I \approx (p_{\perp}/mc)^2 (\omega/2\Omega)$ and the canonically conjugate angle ξ (a combination of wave phase and particle gyrophase) issue from a Hamiltonian \mathcal{K} , given by



$$\begin{aligned}
 \mathcal{K} &= \mathcal{K}_0(I, z) + \mathcal{K}_1(I, z)\sin \xi, \\
 \mathcal{K}_0 &= \eta_z(I - c_2) - \sigma_z s \ell P_0(I, z), \\
 P_0 &= \sqrt{\left(\frac{I - c_2}{s\ell}\right)^2 - 1} - 2\frac{\Omega}{\omega}I.
 \end{aligned}
 \tag{1}$$

The distance z along the field line plays the role of time, so that $d\xi/dz = \partial\mathcal{K}/\partial z$ and $dI/dz = -\partial\mathcal{K}/\partial\xi$. Here ω is the wave frequency, Ω is the (local, unsigned, nonrelativistic) electron gyrofrequency, s is the sign of the particle charge, ℓ is the resonant harmonic number, and η_z is the parallel wave refractive index, $k_{\parallel}c/\omega$. P_0 is the normalized magnitude of p_{\parallel} , where p_{\perp} and p_{\parallel} are components of the physical momentum relative to the background magnetic field. The sign of p_{\parallel} is given by $\sigma_z = \pm 1$. The constant of motion c_2 relates I and the particle kinetic energy E through

$$c_2 = I - s\ell\gamma, \tag{2}$$

where γ is the relativistic factor $1 + E/mc^2$. \mathcal{K}_1 is proportional to the wave amplitude; it is given in detail by Eqs. A2, A4 of Albert (2000), and for the special case of a parallel-propagating wave by Eqs. 2, 3 of Albert et al. (2021). As given in Appendix C of Albert (2000), changes in energy E and equatorial pitch angle α_0 are related to small resonant changes in I by

$$\frac{\Delta E}{mc^2} = \frac{\Delta I}{s\ell}, \quad \Delta\alpha_0 = \frac{\Omega_{eq}/\omega - (\gamma/s\ell)\sin^2\alpha_0}{(p/mc)^2 \sin\alpha_0 \cos\alpha_0} \Delta I, \tag{3}$$

where $\ell \neq 0$, and Ω_{eq} is the equatorial value of Ω .

At a given location z , the resonant value of I is determined to lowest order by $\partial\mathcal{K}_0/\partial I = 0$, which corresponds to the standard resonance condition

$$\omega - k_{\parallel}v_{\parallel} = s\ell\Omega/\gamma. \tag{4}$$

This yields

$$\begin{aligned}
 I_{res} &= c_2 + (s\ell)^2\frac{\Omega}{\omega} + \sigma_z s\ell\eta_z P_{0,res}, \\
 P_{0,res} &= \frac{1}{\sqrt{\eta_z^2 - 1}} \sqrt{1 + 2\frac{\Omega}{\omega}c_2 + \left(\frac{s\ell\Omega}{\omega}\right)^2},
 \end{aligned}
 \tag{5}$$

which generalize Eqs. 5, 6 of Albert et al. (2021) to arbitrary values of $s\ell$. The z dependence of I_{res} is characterized by $\partial I_{res}/\partial\Omega$, which can be written as

$$\frac{\partial I_{res}}{\partial\Omega} = s\ell\sigma_z \frac{\eta_z I_{res} - s\ell\sigma_z P_{0,res}}{\omega(\eta_z^2 - 1)P_{0,res}}. \tag{6}$$

For the prototype situation of an electron ($s = -1$) in primary resonance ($\ell = -1$) and heading toward the equator ($\sigma_z = -1$), as considered here, this quantity is always negative; both z and the gyrofrequency Ω decrease and I_{res} increases. The correspondence between Eq. 1 and the gyro-averaged Lorentz equations of motion was investigated by Albert et al. (2022).

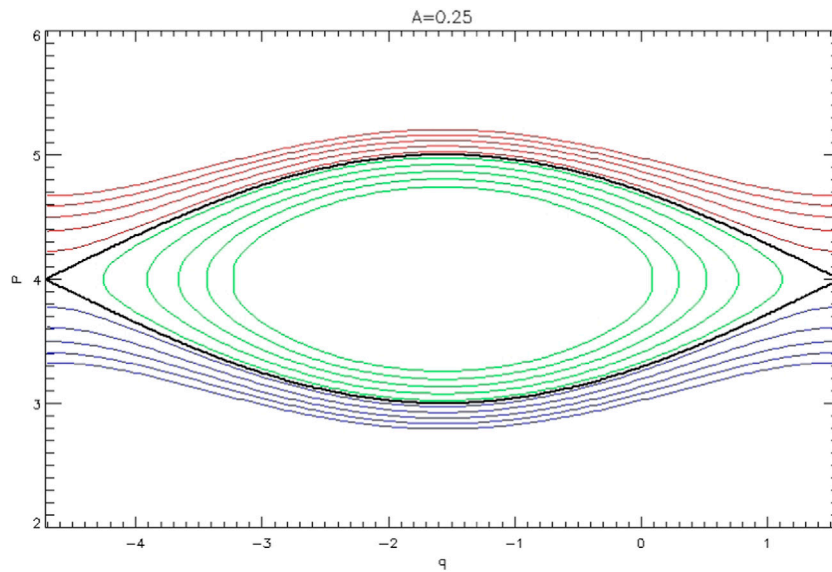


FIGURE 3 Contours of the pendulum Hamiltonian $H(P, q)$ given by Eq. 10, with $A = 0.25$. If the inhomogeneity parameter R is small but positive, the separatrix (shown in black) slowly rises. At resonance near the X -point, particles cross from red contours to blue (phase bunching) or green (phase trapping) contours.

3 Pendulum hamiltonian

A Taylor expansion of \mathcal{K}_0 in Eq. 1 gives the pendulum-like form

$$M(I, \xi, z) = \frac{G_r}{2} (I - I_{res})^2 + F_r \sin \xi \tag{7}$$

where $G_r = \partial^2 \mathcal{K}_0 / \partial I^2$ and $F_r = \mathcal{K}_1$, both evaluated at resonance. Albert (2000) obtained the estimate

$$G_r \approx \frac{\eta_z^2 - 1}{s \ell \sigma_z P_0} \tag{8}$$

It is convenient to define σ_F and σ_G as the signs of F_r and G_r , respectively, so that $F = \sigma_F F_r$ and $G = \sigma_G G_r$ are positive. Then Eq. 7 can be brought into the same form as Equation 72 of Cary et al. (1986) by changing variables to

$$\tau = \sigma_G z, \quad P = GI, \quad q = \xi - \sigma_F \sigma_G \frac{\pi}{2} \tag{9}$$

The equations of motion in these variables are then given by the Hamiltonian

$$H(P, q, \tau) = \frac{1}{2} (P - P_{res})^2 - 2A \sin^2(q/2), \tag{10}$$

with $P_{res} = GI_{res}$ and $A = FG$. Typical contours at fixed $P_{res}(\tau)$ are shown in Figure 3. For the prototype configuration (with $s = \ell =$

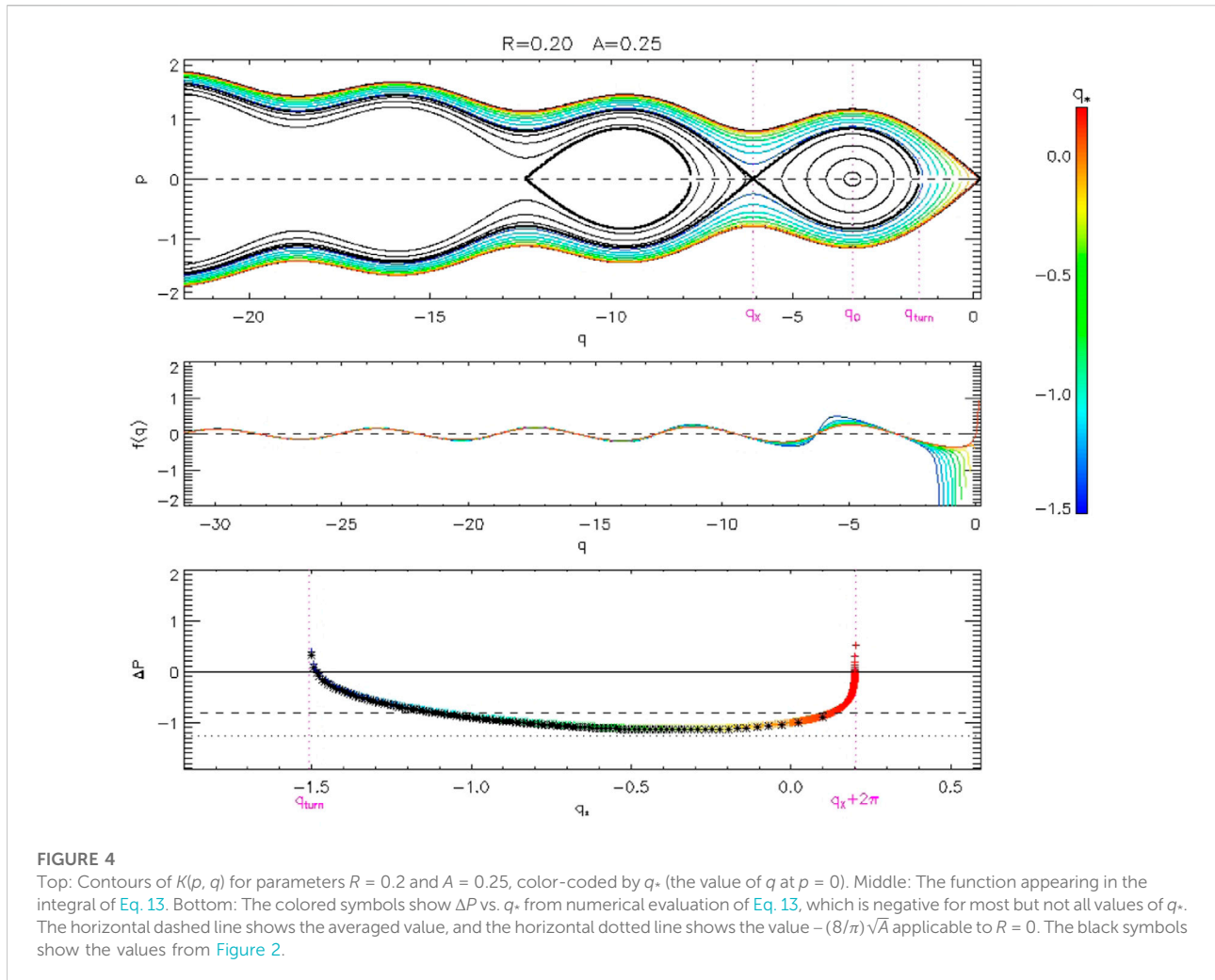
$\sigma_z = -1$) G_r is negative, so $dP_{res}/d\tau = \sigma_G G(dI_{res}/dz)$ is positive. Albert et al. (2021) and Artemyev et al. (2021) considered a more general version of Eq. 7 which retains a factor of \sqrt{I} in the wave term, which can distort the separatrix shape in order to maintain $I > 0$. This can lead to “positive phase bunching” for particles with small initial values of I (Kitahara and Katoh, 2019; Gan et al., 2020). However, as seen in Figure 2, this can occur even in the pendulum approximation.

Transforming from P to $p = P - P_{res}$ in Eq. 10 gives

$$K(p, q, \tau) = \frac{p^2}{2} - A(1 - \cos q - Rq), \tag{11}$$

where both A and the inhomogeneity parameter $R = (dP_{res}/d\tau)/A$ are positive and will be taken as constant. This idealization eliminates the possibility of phase trapping, which involves expansion of the Hamiltonian separatrix to engulf neighboring trajectories.

Trajectories of 120 particles from numerical integration of the equations of motion specified by the Hamiltonian of Eq. 11 are shown in Figure 1, with inhomogeneity parameter $R = 0.1$ and wave amplitude parameter $A = 0.25$. In this case, all values of ΔP are negative. In Figure 2 the wave amplitude parameter A is the same but the inhomogeneity parameter has been increased to $R = 0.2$, resulting in positive ΔP for some values of q at resonance.



4 Integral expression for changes in invariant

Contours of K , from Eq. 11, are shown in the top panel of Figure 4. The linearly unstable X -point obeys $\tan q_x = R/\sqrt{1 - R^2}$ and the stable O -point obeys $\tan q_o = R/(-\sqrt{1 - R^2})$, with the branch choices $-\pi < q_x < -3\pi/2$ and $-3\pi/2 < q_o < -\pi$. The value q_{turn} is the second location where the curve through an X -point crosses $p = 0$, with $q_x < q_o < q_{turn} < q_x + 2\pi$. Finally, q_* refers to where a general trajectory crosses $p = 0$, with $q_{turn} < q_* < q_x + 2\pi$.

The change in P can be expressed as

$$\Delta P = \int dq \frac{dP/d\tau}{dq/d\tau} = \int dq \frac{-\partial H/\partial q}{-\partial K/\partial p} = \int \frac{A \sin q \, dq}{\sqrt{2[K + A(1 - \cos q - Rq)]}} \tag{12}$$

The integral over q is taken from $-\infty$ to the value q_* and then back to $q = -\infty$, where q_* is the value of q as the curve crosses $p = 0$. It is sufficient to integrate from $-\infty$ to q_* and double the result. It is convenient to define $h = (K + A)/AR$ and $a = 1/R$, so that

$$\Delta P = \sqrt{\frac{2A}{R}} \int_{-\infty}^{q_*} \frac{\sin q \, dq}{\sqrt{h - a \cos q - q}} \tag{13}$$

Note that $h(p, q + 2\pi) = h(p, q) + 2\pi$.

This infinite, oscillatory integral is carried out along contours of $h(p, q)$. The middle panel shows values of the integrand, and indicates that a wide range of q values contribute to the total integral. The bottom panel shows numerical evaluations (in color), which are generally negative but can be positive near $q_* = q_{turn}$ or $q_* = q_x + 2\pi$. Also shown, as black symbols, are the values from the simulations of Figure 2. The excellent agreement is expected since Eq. 13 and the equations of motion from Eq. 11 should be exactly equivalent.

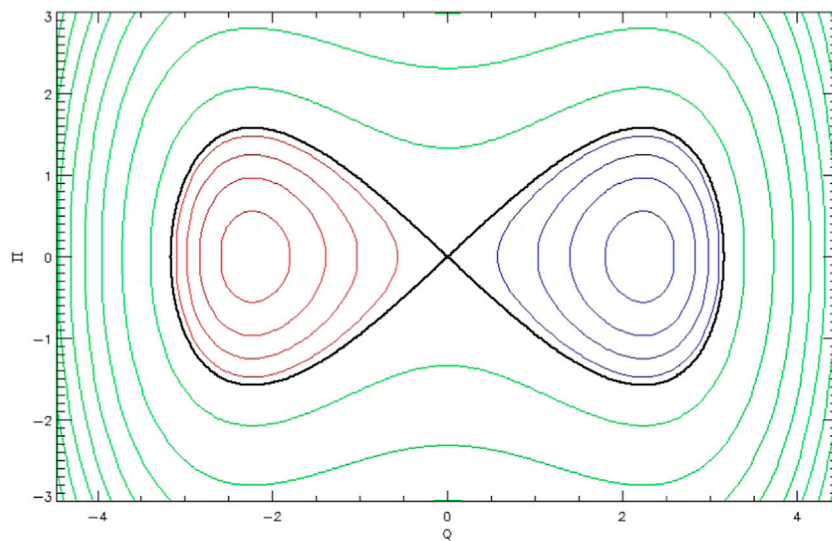


FIGURE 5
Contours of a two-lobe Hamiltonian of the form of Eq. 19. The contour colors correspond to those of Figure 3.

4.1 Average value of ΔP

The integral for ΔP cannot be carried out in closed form, but it can be averaged with respect to q , analytically. Averaging with respect to q is equivalent to averaging with respect to h (Cary et al., 1986; Itin et al., 2000), with the range q_{turn} to $q_x + 2\pi$ corresponding to the range h_x to $h_x + 2\pi$ (since $h_{turn} = h_x$). Following Neishtadt (1999) and Artemyev et al. (2018), the curves are integrated separately over the ranges $q < q_x$ (region 1) and $q > q_x$ (region 2), with the latter combined with the (p, q) island (region 3). For region 1,

$$\begin{aligned}
 I_1 &= \int_{h_x}^{h_x+2\pi} dh \int_{-\infty}^{q_x} \frac{\sin q \, dq}{\sqrt{h - a \cos q - q}} \\
 &= \int_{-\infty}^{q_x} 2dq \sin q \left[\sqrt{h_x + 2\pi - a \cos q - q} - \sqrt{h_x - a \cos q - q} \right] \\
 &= - \int_{q_x-2\pi}^{q_x} 2dq \sin q \sqrt{h_x - a \cos q - q}.
 \end{aligned}
 \tag{14}$$

Next, noting that along the q axis $h \equiv h_0 = a \cos q + q$,

$$\begin{aligned}
 I_2 + I_3 &= \int_{q_x}^{q_x+2\pi} dq \int_{h_0}^{h_x+2\pi} dh \frac{\sin q}{\sqrt{h - a \cos q - q}} \\
 &= \int_{q_x}^{q_x+2\pi} 2dq \sin q \sqrt{h_x + 2\pi - a \cos q - q}.
 \end{aligned}
 \tag{15}$$

Thus $I_1 + I_2 + I_3 = 0$. Finally, I_3 can be expressed as

$$\begin{aligned}
 I_3 &= \int_{q_x}^{q_{turn}} dq \int_{h_0}^{h_x} dh \frac{\sin q}{\sqrt{h - a \cos q - q}} \\
 &= \int_{q_x}^{q_{turn}} 2dq \sin q \sqrt{h_x - a \cos q - q}.
 \end{aligned}
 \tag{16}$$

Writing $\sin q = (a \sin q - 1)/a + 1/a$ leads to $I_3 = S/a$, with

$$S = \int_{q_x}^{q_{turn}} 2dq \sqrt{h_x - a \cos q - q}, \tag{17}$$

which is the area of the (p, q) island. The average of ΔP over regions 1 and 2 is then

$$\langle \Delta P \rangle = -\frac{\sqrt{2AR}}{2\pi} S, \tag{18}$$

which becomes $-(8/\pi)\sqrt{A}$ as $R \rightarrow 0$, in agreement with the estimate obtained by Albert (1993).

5 Two-lobe hamiltonian

Cary et al. (1986) (hereafter CET) gives a comprehensive treatment of adiabatic invariant breaking due to crossing the separatrix of a Hamiltonian $\mathcal{H}(\Pi, Q)$ with the form

$$\mathcal{H}(\Pi, Q, t) = \omega \frac{\Pi^2 - Q^2}{2} + \delta H(\Pi, Q, \epsilon t), \tag{19}$$

where Π and Q are a pair of action-angle variables and the small quantity ϵ indicates that the crossing is slow. This form is chosen to facilitate analysis of motion near the X-point, but Appendix A of CET shows how an arbitrary Hamiltonian may be put into this form to arbitrary order in ϵ (the several typesetting errors in Eq. 10 notwithstanding). The phase portrait of this Hamiltonian has two lobes; typical contours of Eq. 19 are shown in Figure 5.

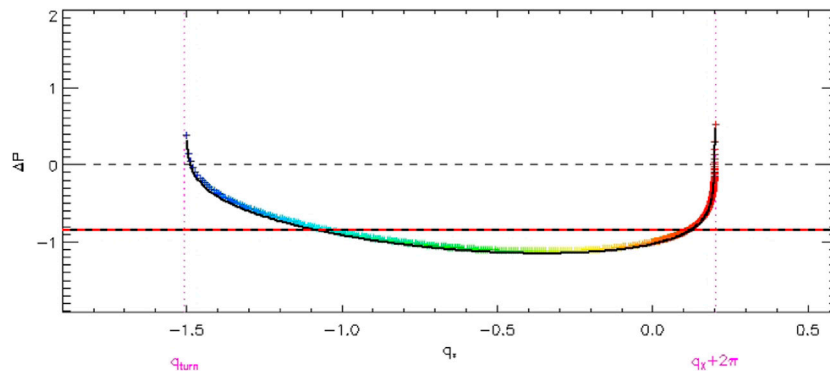


FIGURE 6

The colored symbols show ΔP vs. q_* from Eq. 20, which is negative for most but not all values of q_* . The solid horizontal line shows the averaged value, and the red dashed horizontal line shows the value from Eq. 18. The black symbols show the values from Figure 2. The dotted and dashed vertical lines show the calculated values q_{turn} and $q_x + 2\pi$, respectively, as discussed in the text.

Following a very complex sequence of calculations based on Eq. 19, two special cases are considered, described as symmetric and antisymmetric (which refer to the growth rates of the two lobes shown in 5, not their shapes). The symmetric case was applied to drift orbit bifurcation by Öztürk and Wolf (2007). The antisymmetric case applies to the pendulum Hamiltonian of Eq. 7 and its transformed version Eq. 11, which are of the same form as, respectively, Equation 72 and the subsequent one of CET. With a minor typesetting correction, Equation 84 of CET gives

$$\Delta P = -\frac{8}{\pi}A^{1/2} - \frac{h_0}{\pi A^{1/2}} \log \left| \frac{32A}{h_0} \right| - 2RA^{1/2} \left\{ \left(\frac{1}{2} + \mu \right) \log |\mu| - \log \left| \frac{\Gamma(1 + \mu)}{\sqrt{2\pi}} \right| \right\}, \quad (20)$$

where Equation 75 of CET has been used, and the notation

$$\mu = \frac{h_0}{2\pi RA} \quad (21)$$

has been introduced. Related expressions were presented by Neishtadt (1987). The leading term of Eq. 20 is the same as the estimate of Albert (1993).

To evaluate h_0 and μ in terms of $K(p, q, \tau)$ of Eq. 11, it is necessary to shift K by a constant:

$$h_0(q_*) = K(p = 0, q_*, \tau) - K(p = 0, q_x + 2\pi, \tau), \quad (22)$$

so that $h_0(q_x + 2\pi) = 0$ for consistency with the derivation. It can be shown that $K(q_*)$ is an increasing function of q_* between q_{turn} and $q_x + 2\pi$, so $h_0 \leq 0$, and that μ correspondingly increases from -1 to 0 . Eq. 9 of Tennyson et al. (1986), which was written in terms of $m_d = |\mu|$, is equivalent if $A = \omega = 1$.

Evaluation of Eq. 20 is shown in color in Figure 6. Also shown, as a black curve, are the values from Eq. 13. These two formulations are not exactly equivalent, but are in excellent agreement.

Equation 20 can be approximated near $\mu = 0$ as

$$\Delta P \approx -\frac{8}{\pi}A^{1/2} + RA^{1/2} \log \left| \frac{1}{2\pi\mu} \right|, \quad (23)$$

and near $\mu = -1$ as

$$\Delta P \approx -\frac{8}{\pi}A^{1/2} + 2RA^{1/2} \log \left| \frac{16}{R\sqrt{2\pi^3}} \left(\frac{1}{1 + \mu} - \gamma_0 \right) \right|, \quad (24)$$

where $\gamma_0 \approx 0.5772$ is the Euler constant. For small values of R , these estimates are positive only for very narrow ranges of μ , approximately

$$|\mu| < \frac{1}{2\pi} e^{-8/\pi R} \quad (25)$$

or

$$1 + \mu < \frac{2}{R} e^{-4\pi/R}, \quad (26)$$

respectively. For $R = 0.5$, these values are approximately 10^{-3} and 0.3 , while for $R = 0.2$ they are 5×10^{-7} and 0.02 , respectively. Thus $\Delta P > 0$ only for particles with μ near -1 or extremely near $\mu = 0$.

Equation 20 can be averaged over μ , giving

$$\langle \Delta P \rangle = -\frac{8}{\pi}A^{1/2} \left[1 - \frac{\pi R}{8} \left(1 + \log \frac{16}{\pi R} \right) \right]. \quad (27)$$

This value is shown as the thick black line in Figure 6, and agrees very well with Eq. (18), shown as the dashed red line.

Finally, comparing Eqs. 27, 18 gives the estimate

$$S = \frac{16}{\sqrt{2R}} \left[1 - \frac{\pi R}{8} \left(1 + \log \frac{16}{\pi R} \right) \right], \quad (28)$$

which should be useful in situations where R is slowly changing, and the probability of phase trapping is proportional to the rate of change of S (Artemyev et al., 2018).

6 Summary

Wave-particle interactions are frequently treated with a pendulum Hamiltonian equivalent to Eq. 11. With the wave amplitude parameter A and the inhomogeneity parameter R held constant, phase trapping does not occur, and changes in adiabatic invariant P due to phase bunching are formally expressible by the integral in Eq. 13. This result depends on the wave-particle phase q at resonance; positive values can occur but are uncommon. Averaging over that phase gives the more tractable expression 18, which is always negative.

Equation 20, which is a special case of a detailed analysis of the two-lobe Hamiltonian of Eq. 19, gives the change in P as an explicit function of q at resonance. Its average value, Eq. 27, agrees very well with Eq. 18, and it also accurately reproduces the numerically observed dependence on q , including positive values of ΔP (see Figure 6). Analytical estimates of the fraction of particles with these positive values were obtained, which are exponentially small for small values of R . Finally, combining the two treatments gives a good analytical approximation to the area bounded by the pendulum separatrix, whose rate of increase determines the probability of phase trapping.

Data availability statement

The original contributions presented in the study are included in the article/supplementary material, further inquiries can be directed to the corresponding author.

Author contributions

JMA conceived this work, and wrote and ran the simulations. AA helped analyze approaches to reducing the dimensionality of the system of equations. WL, QM, and LG consulted on the work and made several useful suggestions on the simulations and presentation.

References

- Albert, J. M., Artemyev, A. V., Li, W., Gan, L., and Ma, Q. (2021). Models of resonant wave-particle interactions. *JGR. Space Phys.* 126, e2021JA029216. doi:10.1029/2021JA029216
- Albert, J. M., Artemyev, A., Li, W., Gan, L., and Ma, Q. (2022). Equations of motion near cyclotron resonance. *Front. Astron. Space Sci.* 9, 910224. doi:10.3389/fspas.2022.910224
- Albert, J. M. (1993). Cyclotron resonance in an inhomogeneous magnetic field. *Phys. Fluids B Plasma Phys.* 5, 2744–2750. doi:10.1063/1.860715
- Albert, J. M. (2000). Gyroresonant interactions of radiation belt particles with a monochromatic electromagnetic wave. *J. Geophys. Res.* 105, 21191–21209. doi:10.1029/2000JA000008
- Albert, J. M. (2002). Nonlinear interaction of outer zone electrons with VLF waves. *Geophys. Res. Lett.* 29, 116–1–116–3. doi:10.1029/2001GL013941
- Albert, J. M. (2010). Diffusion by one wave and by many waves. *J. Geophys. Res.* 115, A00F05. doi:10.1029/2009JA014732
- Artemyev, A. V., Neishtadt, A. I., Vainchtein, D. L., Vasiliev, A. A., Vasko, I., and Zelenyi, L. (2018). Trapping (capture) into resonance and scattering on resonance: Summary of results for space plasma systems. *Commun. Nonlinear Sci. Numer. Simul.* 65, 111–160. doi:10.1016/j.cnsns.2018.05.004
- Artemyev, A. V., Neishtadt, A. I., Albert, J. M., Gan, L., Li, W., and Ma, Q. (2021). Theoretical model of the nonlinear resonant interaction of whistler-mode waves and field-aligned electrons. *Phys. Plasmas* 28, 052902. doi:10.1063/5.0046635
- Bortnik, J., and Thorne, R. M. (2007). The dual role of elfvlf chorus waves in the acceleration and precipitation of radiation belt electrons. *J. Atmos. Sol. Terr. Phys.* 69, 378–386. doi:10.1016/j.jastp.2006.05.030

Funding

JMA was supported by NASA grant 80NSSC19K0845 and the Space Vehicles Directorate of the Air Force Research Laboratory. WL, LG, and QM also acknowledge the NASA grants 80NSSC20K1506 and 80NSSC20K0698, NSF grant AGS-1847818, and the Alfred P. Sloan Research Fellowship FG-2018-10936.

Acknowledgments

The views expressed are those of the author and do not reflect the official guidance or position of the United States Government, the Department of Defense or of the United States Air Force. The appearance of external hyperlinks does not constitute endorsement by the United States Department of Defense (DoD) of the linked websites, or the information, products, or services contained therein. The DoD does not exercise any editorial, security, or other control over the information you may find at these locations.

Conflict of interest

The authors declare that the research was conducted in the absence of any commercial or financial relationships that could be construed as a potential conflict of interest.

The handling editor XJZ declared a shared affiliation with the authors AA, QM at the time of review.

Publisher's note

All claims expressed in this article are solely those of the authors and do not necessarily represent those of their affiliated organizations, or those of the publisher, the editors and the reviewers. Any product that may be evaluated in this article, or claim that may be made by its manufacturer, is not guaranteed or endorsed by the publisher.

- Bortnik, J., Thorne, R. M., and Inan, U. S. (2008). Nonlinear interaction of energetic electrons with large amplitude chorus. *Geophys. Res. Lett.* 35, L21102. doi:10.1029/2008GL035500
- Cary, J. R., Escande, D. F., and Tennyson, J. L. (1986). Adiabatic-invariant change due to separatrix crossing. *Phys. Rev. A . Coll. Park.* 34, 4256–4275. doi:10.1103/PhysRevA.34.4256
- Chang, H. C., and Inan, U. S. (1983). Quasi-relativistic electron precipitation due to interactions with coherent VLF waves in the magnetosphere. *J. Geophys. Res.* 88, 318. doi:10.1029/ja088ia01p00318
- Gan, L., Li, W., Ma, Q., Albert, J. M., Artemyev, A. V., Bortnik, J., et al. (2020). Nonlinear interactions between radiation belt electrons and chorus waves: Dependence on wave amplitude modulation. *Geophys. Res. Lett.* 47, e2019GL085987. doi:10.1029/2019GL085987
- Itin, A. P., Neishtadt, A. I., and Vasiliev, A. A. (2000). Captures into resonance and scattering on resonance in dynamics of a charged relativistic particle in magnetic field and electrostatic wave. *Phys. D. Nonlinear Phenom.* 141, 281–296. doi:10.1016/S0167-2789(00)00039-7
- Kitahara, M., and Katoh, Y. (2019). Anomalous trapping of low pitch angle electrons by coherent whistler mode waves. *JGR. Space Phys.* 124, 5568–5583. doi:10.1029/2019JA026493
- Neishtadt, A. I. (1987). On the change in the adiabatic invariant on crossing a separatrix in systems with two degrees of freedom. *J. Appl. Math. Mech.* 51, 586–592. doi:10.1016/0021-8928(87)90006-2
- Neishtadt, A. (1999). “On adiabatic invariance in two-frequency systems,” in *Hamiltonian systems with three or more degrees of freedom. NATO ASI series (series C: Mathematical and physical Sciences)*. Editor C. Simó (Dordrecht: Springer), 533, 193–213. doi:10.1007/978-94-011-4673-9_17
- Omura, Y., Katoh, Y., and Summers, D. (2008). Theory and simulation of the generation of whistler-mode chorus. *J. Geophys. Res.* 113, A04223. doi:10.1029/2007JA012622
- Öztürk, M. K., and Wolf, R. A. (2007). Bifurcation of drift shells near the dayside magnetopause. *J. Geophys. Res.* 112, A07207. doi:10.1029/2006ja012102
- Tennyson, J. L., Cary, J. R., and Escande, D. F. (1986). Change of the adiabatic invariant due to separatrix crossing. *Phys. Rev. Lett.* 56, 2117–2120. doi:10.1103/PhysRevLett.56.2117